RTC of Distributed Residential Batteries for Market Bidding

Benoit Couraud, Merlinda Andoni, Sonam Norbu, Valentin Robu, David Flynn
Smart Systems Group, Heriot-Watt University, Edinburgh, UK

Email: {b.couraud, m.andoni, sn51, v.robu, d.flynn}@hw.ac.uk

***Abstract*—Economic incentives for distributed renewable generation are being reduced, or even removed in many countries, which paves the way for self-consumption. Therefore, residential batteries are becoming more interesting, although there is still a need for cost reduction and revenues diversification to increase their profitability. In this paper, we propose a three-stage real-time control algorithm for residential batteries that includes bidding strategies on the wholesale energy market. This algorithm either applies to a single battery owned by a prosumer, or to a fleet of distributed residential batteries coordinated by an aggregator. In the first stage of the algorithm, an optimal day-ahead or intra-day scheduling of the aggregated storage assets is computed centrally, based on forecasts of market price and aggregated demand and production of the households. In the second stage, a bidding strategy is proposed for day-ahead or intra-day wholesale energy markets. Finally, in the third stage, a real-time control algorithm based on a smart contract allows coordination of residential batteries to maximize self-consumption of local production and ensure that the whole fleet of assets honours the export contracts with the wholesale market. This algorithm is implemented in the case of an aggregator that installs 70 residential batteries in customer premises to maximize his revenues and reduce the bill for the households. Experimentation is done using real minutely data for demand and production. Results indicate that the proposed algorithm increases the aggregator's revenues by 35% compared to a case without residential flexibility, and increases the self-consumption rate of the households by 2. The robustness of the results to forecast errors and to latency in communication is also demonstrated.**

***Index Terms*—Battery management system, distributed generation, linear programming optimization, smart grids**

I. Introduction

ELECTRIC grids are facing important challenges due to an increasing penetration of distributed intermittent generation, and due to new electricity consumption types at the residential level, such as electric vehicles and electric based heating or cooling systems. To address these challenges, power networks first require new control mechanisms at the system level to compensate the reduction of grid inertia [1], but also at the distribution grid level to regulate local voltage. Although technical solutions already exist, ranging from grid infrastructure reinforcement to local Peer to Peer markets, their economic viability is still to be demonstrated. In the same time, economic incentives for renewable energy production such as Feed in Tariffs (FiT) are being removed in most of the countries, making it more challenging for investors to contribute to net zero carbon emissions schemes [2]. This economic context encourages self-consumption of distributed renewable energy production at the residential level, which is greatly facilitated by local storage through residential chemical batteries. Indeed, although the battery cost is still high [3], residential batteries such as Tesla's PowerWall constitute an interesting compromise between cost, ease of installation and maturity to better integrate renewable generation in the distribution grid [4], [5]. However, residential batteries used solely for local storage have a simple payback period above 10 years [6]–[8], reducing the financial interest of such solutions for a home owner. Hence, energy actors propose additional services to residential batteries, such as ancillary services or contribution to wholesale energy markets, which diversifies the sources of revenues from residential batteries, making them more profitable [9], [10].

Indeed, batteries can first be used locally at the household level to reduce the electricity bill of the households by increasing the self-consumption rate when coupled to a small generator such as solar PV or wind turbines or by realizing price arbitrage. In the same time, the same batteries can be used to provide grid services such as frequency regulation [11], [12], or to balance suppliers' portfolios by bidding in wholesale energy markets [13]. However, participation to such services is generally not open to small assets of power below 1 MW [14]. Hence, there is a need to aggregate these residential batteries in order to access wholesale markets. As a consequence, the control of residential batteries becomes a complex task that must deal with opposing local and global objectives: locally, residential batteries control aims to reduce the bill of the households, following a local schedule, whereas the global objective is to maximize the revenues from the wholesale markets, which requires batteries to follow global recommendations.

Battery control for grid applications has been addressed in many research works [15]–[52]. However, most of these works either consider residential batteries with only a local objective [15]–[24], or optimize the control of a large single battery that participates to the wholesale markets [25]–[34]. Hence, they do not address the problem of a fleet of residential batteries contributing to the wholesale markets as an additional revenue source. Furthermore, only a few works are addressing the problem of RTC for economic optimization, which is necessary to ensure the Battery Management System (BMS) will take a good enough decision in real implementation where

demand and production profiles can be very volatile [15], [21], [24], [26], [45]. To the best of our knowledge, there is no previous work considering real-time control (RTC) of distributed residential batteries that participate to the wholesale energy market. In this paper, we address the technical challenges of distributed residential batteries RTC. We propose an algorithm based on Model Predictive Control (MPC) that maximizes local self-consumption and provides optimal market bidding for the whole fleet of distributed batteries. Coordination of the batteries is achieved through a decentralized Smart Contract deployed on a private blockchain with low computational needs.

The main contributions of this paper are:

- A RTC for residential batteries that minimizes the households' electricity bill.
- A wholesale market bidding strategy for an aggregator of residential batteries.
- A Smart Contract to synchronize distributed batteries that participate to wholesale markets.
- A sensitivity analysis that assess the robustness of the algorithm to forecast uncertainties and communication latency.

The structure of the paper is as follows: in section II we provide a literature review on battery control for electrical grid applications. In section III, we present the overall strategy of the proposed algorithm. In section IV we describe the operations required at the aggregator level, whereas the distributed real-time (RT) operations are detailed in section V. In section VI, we implement and study the benefits of the proposed algorithm in the case of 70 residential batteries that participate to the day-ahead wholesale market. Finally, section VII concludes on the relevance of the proposed algorithm to increase the share of renewable energies in the energy mix.

II. Review of Battery Control for Grid Applications

Battery control and smart scheduling constitute an important research area in which the aim is to optimize the revenues and services a battery can provide. Battery control consists of real-time (RT) decisions to charge or discharge a battery at every time step of the Battery Management System (BMS) controller (from μs to ms). This decision can be done with a recommendation from an optimized schedule based on forecast of future production and demand, in which case the control is called *optimisation based control*, or without any recommendation, in which case it is called *heuristic control*. Most of battery control algorithms proposed in research works consist in optimisation based control for a single battery [15]–[18], [25], [27], [31], [34], [35], [37], [41], [42], [44]–[47], [51].

A. Types of control objectives

The aim of the optimization can be categorized into 2 types: *economic optimization* and *grid services optimization*.

- **Economic optimization**: in economic optimization, the goal is to maximize the revenues of the battery owner. This can be done by supporting an intermittent renewable energy system [39], [42], [52] or by using stand-alone batteries to bid on the wholesale markets or to realize energy arbitrage [16], [25], [27], [28], [30]–[34], [49]. Another use of batteries for economic optimization is to reduce the electricity cost of a more comprehensive system that includes distributed production and demand, such as microgrids [15], [17], [19], [24], [29], [38], [45], [48], [51] or residential prosumers [15], [18], [20], [21], [26], [28]. In these economic optimization implementations, the strategy can either be to take advantage of Time of Use (ToU) prices and FiT tariffs [15]–[24] or to provide optimal bidding strategies for wholesale energy markets [17], [25]–[34], [49].
- **Grid services optimization**: in these applications, the objective is to provide optimal services to the grid, either through system frequency regulation [27], [31], [33], [34], [36], [36], [37], [40], [43], [44], [46], [47], [49] or local voltage regulation [36], [40], [41], [48].

B. Real-Time battery control

Once an optimal battery schedule has been computed by the optimization process, some research work propose a real-time control (RTC) algorithm to follow the optimal recommendations. However, most of these RTC algorithms apply to the case of grid services optimisation, for which the strategy mostly consists in following the frequency and variations in power balance, or in following a specific signal from the grid operator [27], [35], [37]–[41], [43], [44], [46], [47]. Indeed, only a few research works addressed the challenges of RTC strategies in economic optimization, although it is an important topic as the optimal schedule often relies on non-perfectly accurate forecasts of the system's demand and production.

RTC has either been implemented through Model Predictive Control (MPC) for close to RT decisions [21], [45], or through heuristic rules for full RT decisions [15], [26]. In [15] and [26], the authors propose a rule based RTC that updates the battery setpoints after comparing RT measurements and forecasts of the net export targets at the Point of Common Coupling (PCC). In [25], the control follows the market price that is updated every 5-minutes interval, and does not exactly qualify for RTC. Similarly, [45] and [21] both provide a Model Predictive Control (MPC) algorithm where the optimization for RT decision is run with a time horizon of one day with 15 minutes time steps. Hence, except for [26] that uses minutely data for their simulations, most of the current research works rely on 15-minutes resolution data.

C. Distributed batteries

Finally, most of the research works that focus on economic optimization problems only consider a single battery or equivalent scenarios in which all batteries either follow the same state of charge, or can communicate in full real-time. There is only a few works that address the case of a fleet of distributed batteries that behave differently [26]. Indeed, coordination of distributed batteries is usually addressed in the case of grid services for local grid regulation [38]–[40], [43],

mostly focusing on smoothing a local load profile, or for larger scale frequency regulation [30], [40]. In these cases, research works either consider that all the assets are synchronized by a signal from the system operator, such as the frequency, or assume a perfect RT communication between the assets, which then corresponds to the case of a single battery. Distributed batteries have also been considered in studies focusing on local energy markets, such as [26] and [35]. In these cases, batteries did not need to synchronize as they did not participate to the system's wholesale markets.

To the authors' best knowledge, there is no research work that address RTC of distributed residential batteries in the case of optimization of the batteries owners' revenues. However, it is now necessary to address this use case in order to diversify the services and sources of revenue for flexibility assets.

III. Control Strategy for Distributed Residential Batteries

In this section, we present the overall control strategy for a fleet of distributed residential batteries in order to optimize local consumption and revenue generation in the wholesale markets.

A. Use case considered

In this study, we address the use case of Energy as a Service, where an energy supplier or aggregator invests in decentralized generation and storage assets installed at end-users premises (residential households or commercial buildings for example). The economic objective of the supplier or aggregator is to maximize his revenues, that come from the bill reduction of the end-users and from the revenues obtained from selling energy in the wholesale market. Other objectives are to increase the penetration of renewable in the energy mix, and to increase local consumption of distributed generation. This corresponds to the scenario of the ReFLEX project [53], one of the largest smart energy demonstrators in the UK - running on the Orkney islands in Scotland.

A visual representation of the use case is proposed in Fig. 1. Assets correspond to residential or commercial buildings loads, rooftop solar PV (Photovoltaic) owned by the home owner or the aggregator (supplier), and residential batteries installed at the end-user premises. Other assets can also be considered such as large PV power plants and wind farms, that can be owned by the aggregator (supplier). The aggregator takes advantage of these assets to bid on the wholesale energy market, from which he will generate revenue. During RT operations, the batteries will also maximize local self-consumption. The coordination of the controllable assets (the batteries) to meet the commitment made on the wholesale markets is achieved through a communication with a dedicated smart contract that will be presented in section V.

B. Overall Strategy

The control strategy can be divided into three main phases that are detailed below and in Fig. 2.

In the first phase, based on price, demand and production forecasts, the aggregator computes the optimal schedule and

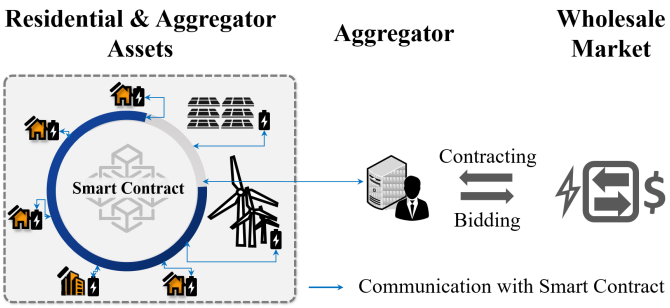

Fig. 1: Use case representation.

revenue he could expect if all the assets were not distributed but aggregated into one large load, one large PV and wind production, and one large battery. The reason for the aggregation of all the assets is to increase the accuracy of the forecasts and reduce the risk to submit unachievable bids to the wholesale market. The steps followed by the aggregator are listed below:

- Forecast of the aggregated load of all the end-users considered in the assets for the next day (or rest of the day).
- Forecast of the aggregated production of all the generation assets (rooftop PV, solar and wind farms) for the next day (or rest of the day).
- Forecast of the future market prices for the next day (or rest of the day).
- Optimization of the schedule of a virtual large battery consisting of the aggregation of all the residential batteries. The optimization process is detailed in section IV

In the second phase, the aggregator use the optimal schedule to determine the forecasted net exports of the aggregated fleet of assets (loads, generations and batteries) for the next considered periods (next day in the case of day-ahead market, or end of the considered day in the case of intra-day market). The aggregator then submits corresponding bids to the wholesale market. Once the market is cleared by the system operator, the aggregator receives export contracts for specific times and energy quantities. If the contracts differ from the bids proposed by the aggregator, he shall re-run an optimization of the schedule of the virtual aggregated battery based on an updated *price* time-series such that the prices of all the time intervals where the aggregator's fleet has not been awarded any contract should be equal to 0. Similarly, export quantities for time intervals in which the aggregator is requested to export energy shall be intervals in which the net export is limited to the energy quantities awarded in the contracts. Finally, the second phase is completed once the aggregator circulates the 3 following time series to the distributed fleet: the optimized SoC profile $SoC^{t,A}$ for the virtual aggregated battery, the required aggregated net export, and the evolution of operating mode (following residual demand or not, where the residual demand consists in the difference between the demand and production of the considered system). This communication can be done directly by direct communication between the aggregator's servers and the distributed batteries, or by storing these time-series into a dedicated smart contract as shown in Fig. 1.

Finally, the third phase corresponds to the RT operations of the distributed batteries. This phase is detailed in section V. Using the 3 time series sent by the aggregator and information from the aggregated fleet sent by the smart contract and updated every 5 to 15 min, every battery follows a Model Predictive Control (MPC) algorithm to determine the RT operations. As all BMS in the market are not able to achieve optimization, we also propose an equivalent rule-based algorithm. Coordination among all the residential batteries is achieved through the smart contract. The smart contract first ensures that the whole fleet will export the required net export as agreed on the wholesale market. Then, the smart contract allows a redistribution of extra energy when some households produce more power than they can consume locally. The details of the RT operations are presented in section V.

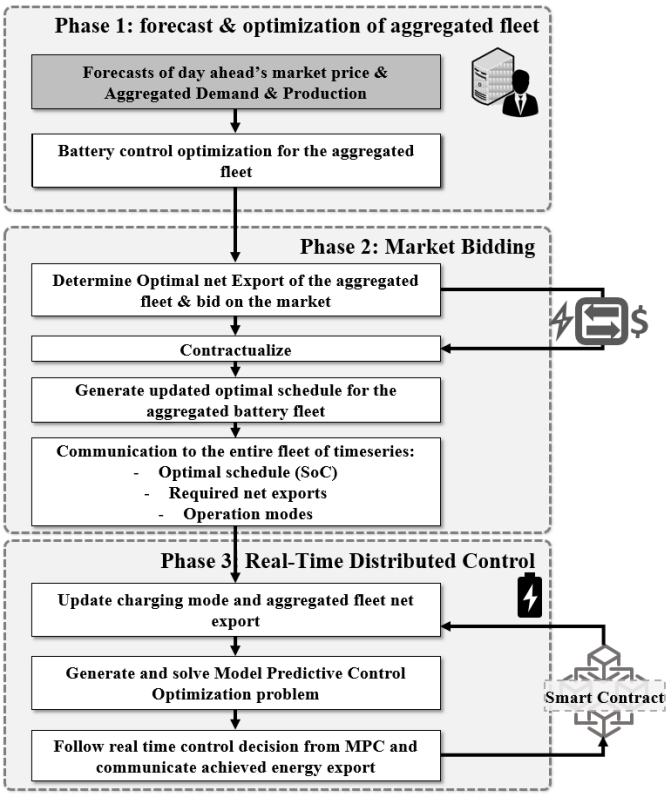

Fig. 2: Overall strategy for the control of distributed batteries contributing to the wholesale market.

IV. Centralised Optimization and Market Bidding

In this section, we detail the content of phases 1 and 2 that are carried by the aggregator in a centralized way, by aggregating all the assets. Hence, in this section, the aggregator acts as if there was only one aggregated load, one aggregated generation (PV and Wind) and one large battery.

A. Optimization of the schedule for the aggregated assets

Before submitting a bid in the day-ahead or intra-day markets, the aggregator aims to determine the optimal net export he can expect to meet in each of the market time intervals of the considered next period (next day in the case of day-ahead market). To do so, the proposed framework includes an optimization process in which the aggregator optimizes the possible revenues of the aggregated fleet. The optimization problem to be solved is described in the following optimization problem [7], for which each time interval t corresponds to the wholesale market intervals (30 minutes intervals in Europe).

$$\begin{aligned} \underset{E^t_{B^A_D}, E^t_{B^A_C}, \forall t}{\text{minimize}} \quad & \sum_{t=1}^{T} E^t_{i^A}\pi^t_i - E^t_{e^A}\pi^t_e \\ \text{subject to} \quad & (2),\ (3) \\ & E^t_{B^A_D}, E^t_{B^A_C}, E^t_{i^A}, E^t_{e^A} \ \geq 0,\ \forall t. \end{aligned} \tag{1}$$

where $E^t_{B^A_D}, E^t_{B^A_C}$ are the discharged and charged energies of the aggregated battery in time interval t respectively, $E^t_{i^A}$ and $E^t_{e^A}$ are respectively the net import and export of the aggregated fleet of assets (loads, production and batteries) to the grid in time interval t. π^t_i is the electricity retail price that the end-users pay when importing electricity from the grid and π^t_e is the forecasted wholesale market price for time interval t. Constraint equation (2) corresponds to the energy balance so demand is met at all time:

$$\begin{aligned} E^t_{i^A} + \eta_d E^t_{B^A_D} - \frac{E^t_{B^A_C}}{\eta_c} &= E^t_{D^A} - E^t_{P^A} \\ E^t_{e^A} - \eta_d E^t_{B^A_D} + \frac{E^t_{B^A_C}}{\eta_c} &= E^t_{P^A} - E^t_{D^A} \end{aligned} \tag{2}$$

where η_d and η_c are the discharging and charging efficiencies of the battery, respectively, and $E^t_{D^A}$ and $E^t_{P^A}$ are the forecasted energy demand and production respectively of the whole portfolio of the aggregator (end-users' loads and generation assets such as PV and Wind). Then, (3) expresses the state of charge (SoC) limits for the aggregated battery and applies to every time interval t.

$$SoC^A_{min} \leq \sum_{n=1}^{t} \left(E^n_{B^A_C} - E^n_{B^A_D} \right) + SoC^{0,A} \leq SoC^A_{max} \tag{3}$$

The details of the auxiliary and binary variables for this Mixed Integer Linear Programming problem are proposed in [7], whereas the process to generate the wholesale market price, the aggregated load and production forecasts is beyond the scope of this paper.

This optimization problem must be solved at two different stages of the proposed strategy. First in phase 1, to generate the net export $E^t_{e^A}$ of the whole fleet for every market interval t, that will be used in the bidding process. Then, this optimization problem shall be solved again in phase 2 once the aggregator has been awarded export contracts. In this second optimization, the wholesale market price π^t_e shall be updated to match the cleared market price in time intervals where a contract was awarded to the aggregator, and $\pi^t_e = 0$ for every time interval t in which the aggregator does not have any export requirement. Similarly, the net exported energy constraints $E^t_{e^A}$ must be updated such that $E^t_{e^A} = E^t_c$ for every time interval t where an export contract was awarded, with E^t_c the net export energy quantity for time interval t

that is required by the contractual agreement with the system operator.

B. Market bidding process

The bidding process consists in submitting a bid to the market operator for every time interval considered. A bid consists in an energy quantity and a price. Once the aggregator solved the optimization problem in phase 1, he obtains a time serie $E^t_{e^A}$ that corresponds to the possible net energy exports for every time interval. Instead of using directly these energy quantities as bids on the market, in this study we propose to first smooth the optimized time serie $E^t_{e^A}$. Indeed, in order to keep the simplicity of the proposed MILP problem, no constraints (and corresponding auxiliary variables) were added to limit the variability of the battery charge and discharge. Hence, the obtained optimal variables such as $E^t_{B^A_C}, E^t_{B^A_D}$ and $E^t_{e^A}$ might have important variations between two consecutive similar intervals. This can happen when the wholesale market price forecasts have exact same values for several consecutive market intervals. In order to smooth the obtained variables, we propose to simulate (run) the RTC algorithm proposed in section V for the aggregated battery, using the SoC and export recommendations from this imperfect first optimization results and the forecasted demand and production. The net energy exports time serie obtained from this RT simulation can then be used as the bids quantities submitted to the wholesale market. The computation of the price of each bid depends on the type of market clearing process (type of auction), and is beyond the scope of the paper.

C. Control of distributed batteries

At the end of the bidding period, the market operator clears the market, and awards stakeholders with export contracts they must honour. The aggregator of distributed assets must then ensure that all assets will contribute to the export commitment so the export contracts are honoured. Meanwhile, the aggregator must maximize self consumption at local levels in order to minimize the households' bills by limiting the imports of each household, and must consider that batteries cannot be synchronized in full RT. Indeed, communication intervals between residential batteries and a central server is usually above 5 min. Hence, batteries cannot be considered as a unique battery. Therefore, the RTC strategy consists in letting the batteries manage themselves their RT operations, while following recommendations from the aggregator. Recommendations that are needed at the local level consist in the following time series, that are sent only once after a new export contract is received:

- The computed optimal charging/discharging profile for the aggregated battery as a State of Charge $SoC^{t,A}$ expressed in % (time-series).
- The required net export energy quantities for the aggregated fleet, which corresponds to the awarded contracts (time-series).
- A *state indicator*, noted $\mathcal{S}$, that represents the mode of operation of the aggregated battery for every time interval: it equals 0 if the battery should follow the net import/export of the end-users (loads and renewable generations) and 1 otherwise:

$$\mathcal{S} = \begin{cases} 0, & \text{if Battery follows residual demand.} \\ 1, & \text{otherwise.} \end{cases} \quad (4)$$

Hence, the aggregator only communicates once with the distributed batteries in order to broadcast the optimal profiles of the virtual aggregated battery. Then, distributed batteries will run the RT algorithm presented in the next section, and will coordinate with each other using the smart contract deployed on a blockchain dedicated to this purpose.

V. Real-Time Control of Distributed Batteries

The third phase of this control algorithm corresponds to the real-time control (RTC) algorithm that runs in every battery's BMS. On top of the algorithm running in the BMS, a smart contract is implemented to coordinate the exports and imports from all the households. In this section, we detail the RTC algorithm and the smart contract implementation.

A. RTC Algorithm

Due to different computing or implementation capabilities of BMS, two different approaches have been considered: one based on Model-Predictive Control (MPC), and another one, rule based control that is a simplified version of the MPC. They are both detailed in this subsection, although only one needs be implemented in a BMS.

1) Model-Predictive Control: In the MPC approach, each BMS solves a local optimization problem at regular time interval t_j (e.g. $t_{j+1} - t_j = 2$ min in our simulations). The optimization problem computes the optimal battery schedule for the rest of the market time interval. Within the time between two consecutive optimizations, for every time step t_s of the BMS (in the range of 200 μs), the BMS operation will follow the recommendation from the optimal schedule. This recommendation is either to follow the local residual demand, or to apply a specific charge/discharge power given in the first steps of the schedule computed in the MPC optimization.

Fig. 3 details the chronology of the MPC algorithm. At every beginning of a new market time interval t, the BMS initializes $RE^{t,A}$ (the remaining net export required from the whole fleet) with the value that was communicated originally by the aggregator. For intervals where no contract was agreed, $RE^{t,A} = 0$. Then, at every communication time interval with the smart contract, each BMS receives an updated value of $RE^{t,A}$, the remaining net export required from the whole fleet, that can be negative if the fleet produced more than what was needed.

Along with $RE^{t,A}$, the smart contract communicates 2 weights w^k_e and w^k_i to each battery k, that represent the percentage of $RE^{t,A}$ that should be exported (w^k_e if $RE^{t,A} > 0$) or imported (w^k_i if $RE^{t,A} < 0$) by the battery k within the rest of time interval t. Hence, using w^k_e and w^k_i communicated by the smart contract during the previous communication, each

$$\begin{aligned} \underset{E^l_{B^k_D}, E^l_{B^k_C}, \forall l}{\text{minimize}} \quad & \sum_{l=t_{j+1}}^{t} E^l_{i^k}\pi^l_i + (1-\varepsilon_{RE})E^l_{e^k}\pi^l_e + \mathcal{S}^t(1-\varepsilon^2_{RE})\frac{SoC^{t,A}-SoC^{t,k}}{SoC^k_{max}} + \varepsilon_{RE}\frac{\left|RE^{t,k} - \sum_{l=t_{j+1}}^{t}\left(E^l_{e^k}-E^l_{i^k}\right)\right|}{E_{max}} \\ \text{subject to} \quad & (2),\ (3) \\ & E^l_{B^k_D}, E^l_{B^k_C}, E^{i^k}_l, E^l_{e^k} \geq 0,\ \forall l. \end{aligned} \tag{6}$$

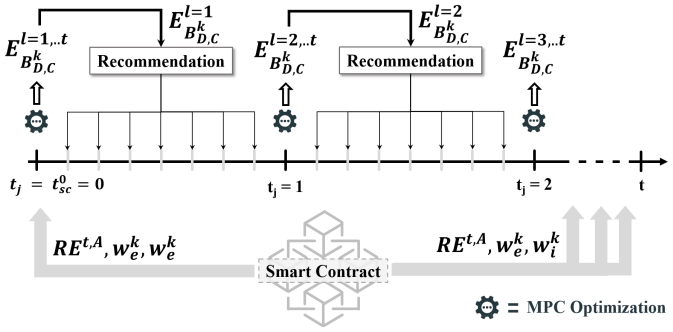

Fig. 3: MPC process showing a case where the smart contract communicates the remaining energy quantity and the battery's weight coefficients at the beginning of the market interval and every 5 minutes afterwards. Similarly, the BMS regularly communicates its state of charge and the exported energy to the smart contract (not displayed).

BMS updates $RE^{t,k}$, the remaining net export required from the battery k before the end of the market interval.

$$RE^{t,k} = \begin{cases} RE^{t,A}\cdot w^k_e - \sum_{l=t_{sc}}^{t_j}\left(E^l_{e^k} - E^l_{i^k}\right), & \text{if } RE^{t,A} \geq 0 \\ RE^{t,A}\cdot w^k_i - \sum_{l=t_{sc}}^{t_j}\left(E^l_{e^k} - E^l_{i^k}\right), & \text{otherwise.} \end{cases} \tag{5}$$

where $RE^{t,A}$ is the remaining net export required from the whole fleet, sent to the battery's BMS at time t_{sc}. It is positive when the assets are asked to export energy, and negative when the fleet has exported too much energy. w^k_e and w^k_i correspond to the percentage of the remaining net export of the whole fleet that should be carried by battery k. w^k_e applies if the fleet needs to export energy, whereas w^k_i applies if the aggregated fleet exported too much energy and needs to import back energy in order to achieve E^t_c, the contractual energy quantity for this time interval t. There are 5 time indicators to be considered. T, the larger, is the time horizon taken for the optimization run by the aggregator. For example T corresponds to a 24 hours period in the case of the day-ahead market. Then t corresponds to the current market time interval (for example $t-(t-1) = 30$ min). Then, t_{sc} is the time at which the BMS received the last information from the smart contract. In the case of a communication time interval of 5 minutes, $t_{sc}-t_{sc-1} = 5$ min. t_j corresponds to the time at which the optimization happens (every 2 minutes for example). Finally, the smallest time step t_s corresponds to the cycle time for BMS operations (for example, $t_s - t_{s-1} = 200\ \mu$s). Hence, $\sum_{l=t_{sc}}^{t_j}\left(E^l_{e^k} - E^l_{i^k}\right)$ corresponds to the effort (export or import) that was already realized by the household k since the last set point $RE^{t,A}$ sent by the smart contract.

Along with $RE^{t,k}$, the BMS computes a forecast of the household's consumption and production in the rest of the current market interval. In our simulations, market time interval is equal to 30 minutes, and the BMS generates a forecast with 15 min time steps for the remaining time in the market interval. Although forecast algorithms are beyond the scope of this paper, our experiments showed that Linear Regression Forecasting demonstrated the best compromise between accuracy and computational speed for forecasts of up to 1 hour ahead. Beyond this forecasting horizon, K-Nearest Neighbour regressions showed better accuracy results.

In order to optimize the bill of the households, we propose a local optimization problem to determine the residential battery schedule that minimizes the cost of electricity consumption of the household. Unlike the optimization given in section IV that only focused on optimization the aggregator's revenues, the objective function of the MPC optimization also includes the SoC and net export requirements from the aggregator and smart contract. However, it is good practice to make sure that the SoC target $SoC^{t,A}$ and net export target $RE^{t,k}$ are achievable. Hence, it is necessary to coerce them to achievable values given the local consumption and production forecasts. The optimization problem solved in the MPC is shown in (6), where t represents the time at the end of the market time interval, $t_j \in [0,t]$ is the time at which the optimization is run, ε_{RE} corresponds to a state variable such that $\varepsilon_{RE} = \text{sgn}(RE^{t,k})$, and $\mathcal{S}^t$ is the battery state indicator for time interval t as sent by the aggregator after the contractual agreement. $SoC^{t,k}$ is the state of charge of the k^{th} battery at the end of time interval t. $RE^{t,k}$ is updated before every optimization (6) using (5). Finally, $\left(E^l_{e^k} - E^l_{i^k}\right)$ corresponds to the net export from household k at time $t_j = l$, and is determined from (2), where t must be replaced by l, and superscript A replaced by k.

As for (1), the problem corresponds to a MILP formulation where the absolute value in (6) is achieved by introducing an auxiliary variable x that replaces the expression $\left|RE^{t,k} - \sum_{l=t_{j+1}}^{t}\left(E^l_{e^k} - E^l_{i^k}\right)\right|$ in the objective function (6), and requires the following constraints:

$$\begin{cases} x \geq RE^{t,k} - \sum_{l=t_{j+1}}^{t}\left(E^l_{e^k} - E^l_{i^k}\right) \\ x \geq \sum_{l=t_{j+1}}^{t}\left(E^l_{e^k} - E^l_{i^k}\right) - RE^{t,k} \\ x \geq 0 \end{cases} \tag{7}$$

The solution of the optimization consists in an optimal battery schedule given by $E_{B_D^k}^{l=t_{j+1},\dots,t}$, $E_{B_C^k}^{l=t_{j+1},\dots,t}$. In the case where the time between two consecutive time steps t_j and t_{j+1} in (6) is one minute, this schedule corresponds to discharging or charging energy quantities for every minute, which is not RT operation. Therefore, as it is shown in Fig. 3, the BMS uses the first charging and discharging energy quantities $E_{B_C^k}^{l=t_{j+1}}$ and $E_{B_D^k}^{l=t_{j+1}}$ to provide a recommendation for the battery power of every time step t_s of the BMS operation between t_j and t_{j+1}. The BMS compares the battery charging/discharging energy $E_{B_C^k}^{t_{j+1}} - E_{B_D^k}^{t_{j+1}}$ with $E_{P^k}^{t_{j+1}} - E_{D^k}^{t_{j+1}}$ the residual demand of household k in order to determine the battery action ($P_{B^k}^s$) for every time step t_s between t_j and t_{j+1}. $P_{B^k}^s$, corresponds to the power of the battery cells, and is positive when the battery is charging, and negative when the battery is discharging. Battery's RT actions are either to follow the residual demand or to follow the recommended power, as shown below:

$$P_{B^k}^s = \begin{cases} \eta\left[P_{P^k}^{t_s} - P_{D^k}^{t_s}\right], & \text{if } E_{B_C^k}^{t_{j+1}} - E_{B_D^k}^{t_{j+1}} = \eta\left[E_{P^k}^{t_{j+1}} - E_{D^k}^{t_{j+1}}\right] \\ \frac{E_{B_C^k}^{t_{j+1}} - E_{B_D^k}^{t_{j+1}}}{s \cdot N_s}, & \text{otherwise.} \end{cases} \tag{8}$$

where N_s is the number of RT actions between t_j and t_{j+1}, s is the time between two consecutive RT actions ($s = t_s - t_{s-1}$), and η is given below:

$$\eta = \begin{cases} \eta_c, & \text{if } P_{P^k}^{t_s} - P_{D^k}^{t_s} \geq 0 \\ \frac{1}{\eta_d}, & \text{Otherwise.} \end{cases} \tag{9}$$

Current BMS are not always able to implement MPC control, either because of computational limitations, or because the manufacturers' Application Programming Interface (API) does not allow optimization. Also, the average CPU (Central Processing Unit) time to solve the MILP described above is 15 ms with an i5 CPU at a frequency of 1.7 GHz, which might be a limitation in some applications where optimizations are needed more frequently. Finally, MPC relies on forecasts generated at the household level, which require further development, computational capability and storage. For these reasons, we also propose an alternative rule-based RTC inspired by the MPC implementation, that is implementable in most of BMS APIs.

2) Rule based RTC: The rule based RTC follows the same logic as the MPC algorithm and aims to increase self-consumption while honouring the export contract with the wholesale market and while following the SoC recommendations $SoC^{t,A}$. Fig. 4 presents the different steps of the algorithm.

The inputs for this RTC algorithm are the same as for the MPC algorithm (time series of the state of charge targets $SoC^{t,A}$, the required net exports E_c^t, the state indicator $\mathcal{S}^t$, the remaining energy need for the fleet $RE^{t,A}$ and the 2 weights w_i^k and w_e^k), along with E_a, which is sent by the smart contract and corresponds to the sum of extra energy quantities that could not be consumed locally by residential batteries because of battery power or capacity limits. The algorithm

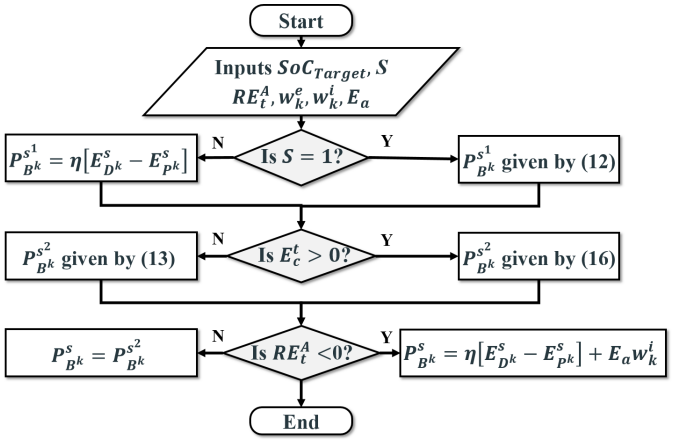

Fig. 4: Process of the rule-based algorithm embedded within BMS.

follows three main steps at every time step t_s of the BMS RT operations:

- Step 1: if the aggregated battery operating state (communicated on the previous day by the aggregator) is $\mathcal{S}^t = 0$, which means that the batteries power must match the residual demand in time interval t, then the BMS computes the first component of its RT operation $P_{B^k}^{s^1}$:

$$P_{B^k}^{s^1} = \eta\left[P_{D^k}^{t_s} - P_{P^k}^{t_s}\right] \tag{10}$$

where $P_{D^k}^{t_s} - P_{P^k}^{t_s}$ are the power consumed and produced at the household level at time t_s.
Similarly, if $\mathcal{S}^t = 1$, this means the aggregated batteries schedule should not match the aggregated residual demand. This can be because the battery fleet must take advantage of a low ToU price to charge, or take advantage of a high price on the wholesale market to discharge. In this case, the battery RT operations should achieve a SoC equal to $SoC^{t,A}$ at the end of the time interval t. Similar to a MPC algorithm, this rule based algorithm computes a schedule of operations between time t_s and t that ensures the SoC target will be met. This schedule must ensure the battery will be charged/discharged with an energy $E^1 = SoC^{t,A} - SoC^{t_{s-1},k}$ before the end of the time interval t. Different approaches can be used to achieve this goal: charge/discharge the battery at maximum power from time t_s until the SoC target $SoC^{t,A}$ is achieved, or charge/discharge the battery at an average power for the whole time $t - t_s$, or use a predetermined profile, such as a ramp-based profile. In this algorithm, we use the latter, in order to reduce the impact of battery operations on the grid a explained below. Fig. 5 shows the adopted shape of power schedule to achieve the energy quantity E^1. It consists of a constant rate increase of the charging/discharging power until the time t_1 is reached, from which the battery needs to charge/discharge at full power in order to meet the target $SoC^{t,A}$. This profile is updated at every time step t_s in order to account for the battery capacity change in the previous time step. Indeed, due to the net export requirements and the local

$$t_1^1 = \frac{2}{\eta_{c,d} E_{\max} - E^{t_{s-1}}} \left[\eta_{c,d} E_{\max} \left(t - \frac{t_s - 1}{2} \right) - E^{t_{s-1}} \frac{t_s + 1}{2} + |E^p| - |E^1| \right] \tag{11}$$

$$P_{B^k}^{s^1} = \begin{cases} P_{B^k}^{(s-1)^1} + 2 \frac{\left[E^1 - E^p - E^{t_{s-1}} (t - t_s) \right]}{s(t-t_s)(t-t_s+1)} & \text{if } t_1^1 \geq t \\ \varepsilon_{E^1} \min \left\{ \frac{E_{\max}}{s}, P_{B^k}^{(s-1)^1} + \frac{\left[\varepsilon_{E^1} \eta E_{\max} - E^{t_{s-1}} \right]^2}{s \left| \varepsilon_{E^1} \eta E_{\max} (2t+1-2t_s) - E^{t_{s-1}} + 2(E^p - E^1) \right|} \right\} & \text{Otherwise} \end{cases} \tag{12}$$

$$t_1^2 = \frac{2}{\eta_{c,d} E_{\max} - E_e^{t_{s-1}}} \left[\eta_{c,d} E_{\max} \left(t - \frac{t_s - 1}{2} \right) - E_e^{t_{s-1}} \frac{t_s + 1}{2} + RE^{t,k} \right] \tag{14}$$

$$P_e^s = \begin{cases} P_e^{s-1} + 2 \frac{\left[RE^{t,k} - E_e^{t_{s-1}} (t - t_s) \right]}{s(t-t_s)(t-t_s+1)} & \text{if } t_1^2 \geq t \\ \varepsilon_{E_c^t} \min \left\{ \frac{E_{\max}}{s}, P_e^{s-1} + \frac{\left[\eta \varepsilon_{E_c^t} E_{\max} - E_e^{t_{s-1}} \right]^2}{s \left| \eta \varepsilon_{E_c^t} E_{\max} (2t+1-2t_s) - E_e^{t_{s-1}} + 2(RE^{t,k}) \right|} \right\} & \text{Otherwise} \end{cases} \tag{15}$$

consumption/production, steps 2 and 3 might modify the operation of the battery, which might charge/discharge the battery at a power $P_{B^k}^s \neq P_{B^k}^{s^1}$. This is similar to the MPC algorithm for which the optimal schedule is recomputed at every time step t_j. The profile displayed in Fig. 5 allows the BMS to give priority to local production in order to achieve E^1. Indeed, instead of first charging from the grid at full power and then injecting back to the grid the energy surplus from local production, we follow a safe profile that will charge from the grid as little as possible until charging from the grid or injecting power to the grid are the last options to meet $SoC^{t,A}$.

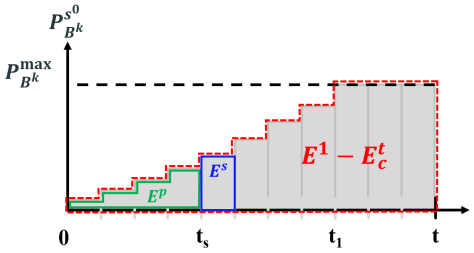

Fig. 5: Proposed operation profile to achieve an energy quantity E^1 for battery k. At every time step t_s, each battery computes the time t_1 from which it must produce its maximum power $P_{B^k}^{\max}$, and then computes the energy that is required for each of the following time step E^s, based on the energy that was already produced E^p.

The time t_1^1 (where superscript 1 corresponds to the step 1 of the rule based algorithm) at which the battery must start to operate at full power is given by (11), where $E_{\max} = sP_{B^k}^{\max}$ is the maximum energy the battery k can output within a time step t_s, $E^{t_{s-1}}$ is the charging/discharging energy realised in the previous timeslot t_{s-1}, E^p is the charged/discharged energy that was realized so far.

Then, the battery power recommendation from the step 1 for the time interval t_s is given by (12), where ε_{E^1} corresponds to the sign of E^1, $P_{B^k}^{(s-1)^1}$ is the battery's power during the previous time step.

- Step 2: once $P_{B^k}^{s^1}$ has been computed, the BMS considers the initial net export requirement for the whole fleet at the considered time interval t, that is known from the initial aggregator's communication after the market was cleared. If there is no export contract for time interval t, the battery power recommendation from step 2 follows the charge/discharge recommendation from step 1. However, it must also take advantage of the local production and consumption. Hence, if there is no contract for time interval t ($E_c^t = 0$), the battery power after step 2 is given by (13).

$$P_{B^k}^{s^2} = \begin{cases} \max \left\{ P_{B^k}^{s^1}, \eta \left[P_{D^k}^{t_s} - P_{P^k}^{t_s} \right] \right\} & \text{if } P_{B^k}^{s^1} \geq 0 \\ \min \left\{ P_{B^k}^{s^1}, \eta \left[P_{D^k}^{t_s} - P_{P^k}^{t_s} \right] \right\} & \text{if } P_{B^k}^{s^1} < 0 \end{cases}, \mathcal{S}^t = 0 \tag{13}$$

If there is an export contract for time interval t ($E_c^t > 0$), the RT algorithm must ensure this contract is honoured. Similar to the MPC algorithm, at every time step t_{sc}, the smart contract sends an updated value of $RE^{t,A}$, the remaining energy to be exported by the whole fleet in order to honour the contract, along with w_k^e the weight that states the contribution of battery k in the production of $RE^{t,A}$. Hence, each battery k can compute $RE^{t,k}$ the amount of energy it should export in order to meet the global target E_c^t. Similar to the step 1, there are different strategies to reach this target ($RE^{t,k}$). The battery can either produce its maximum power until it has exported $RE^{t,k}$, or exporting a constant power during the rest of the time interval in order to reach $RE^{t,k}$ at the end of time interval t, or use a predetermined ramping profile. As for step 1, we adopted the latter option in order to reduce the impact of the battery on the grid. Hence, at every time step t_s, each battery computes a schedule of energy exports of the household required to reach the target $RE^{t,k}$ that follows the shape proposed in Fig. 5. The time t_1^2 corresponds to the time from which the battery needs to export its maximum power in order to meet the target $RE^{t,k}$, where superscript 2 corresponds

to step 2. It is given by (14), where $E_e^{t_{s-1}} = s \cdot P_e^{s-1}$. P_e^s is the required export power from household k at time t_s in order to achieve the net export $RE^{t,k}$. It is given in (15), with $\varepsilon_{E_c^t} = sgn(E_c^t)$. It is worth noting that P_e^s is not the battery power, but the export power that is required at time t_s from the whole household k in order to meet the target $RE^{t,k}$. Once P_e^s has been computed, the battery RT operation setpoint can be determined by using the following expression:

$$P_{B^k}^{s^2} = P_{B^k}^{s^1} + \eta \min\left\{0, P_{P^k}^{t_s} - P_{D^k}^{t_s} - P_{B^k}^{s^1} - P_e^s\right\}. \tag{16}$$

- Step 3: finally, the last step takes into account any energy surplus that may have been exported by the aggregated fleet. Indeed, if there has been too much energy exported by the fleet, then batteries should charge in order to reduce the mismatch between the agreed export and the achieved export. Hence, the BMS determines the final battery power $P_{B^k}^s$ for time step t_s using the expression below:

$$P_{B^k}^s = \begin{cases} P_{B^k}^{s^2} & \text{if } RE^{t,A} \geq 0 \\ \eta\left[P_{P^k}^{t_s} - P_{D^k}^{t_s}\right] + \eta_c w_i^k \frac{E_a}{s} & \text{Otherwise.} \end{cases} \tag{17}$$

where E_a corresponds to the quantity of extra energy produced by the fleet that is available to be consumed at a lower cost by the rest of fleet. It is communicated by the smart contract at every time step t_{sc}. It consists in the sum over the whole fleet of energy injected into the grid as it could not be consumed locally by batteries that are either already full or already charged at maximum power.

3) Communication requirements: As presented in the previous subsection each battery BMS requires external information to operate. First, the BMS requires the time series directly generated by the aggregator after each aggregated optimization (1) and contractual agreement from the wholesale market (once every day if only day-ahead markets are considered). These time series are:

- The aggregated batteries SoC target ($SoC^{t,A}$ $\forall t$) expressed between 0 and 100%.
- The net export energy quantities for the whole fleet E_c^t $\forall t$, with $E_c^t = 0$ if there is no contractual agreement for time interval t.
- The state indicator $\mathcal{S}^t$ $\forall t$ given by (4).

Then, the BMS requires RT communication with the smart contract (at every time t_{sc}) in order to meet the net export requirements E_c^t. The time interval of this RT communication can be between 1 and 15 min for market time intervals of 30min. The communication from the smart contract to the batteries include the following information:

- $RE^{t,A}$ the remaining aggregated energy to be exported in order to meet the fleet's net export contractual agreement E_c^t. It can be negative if the fleet exported more energy than required.
- w_e^k the current percentage of $RE^{t,A}$ that is required to be exported by household k, such that $\sum_{k\in\text{households}} w_e^k = 1$.
- w_i^k the current percentage of $RE^{t,A}$ (when $RE^{t,A} < 0$ or E_a in the case of rule based RT control) that is available to be imported by household k, such that $\sum_{k\in\text{households}} w_i^k = 1$.
- E_a (for the rule based algorithm only) the available extra energy that some households could not consume locally, and that other households' batteries could use to recharge.

Similarly, the in order to generate these information, the smart contract requires inputs from all the households k at every time t_{sc}:

- $E_{D^k}^{t_{s-1}} - E_{P^k}^{t_{s-1}}$ the residual demand from household k during the last operating cycle t_{s-1}.
- $SoC^{t_{sc},k}$ the SoC of the battery k at the time of the communication.
- $E_e^{t_{sc},k}$ the energy exported by household k since the last communication with the smart contract t_{sc-1}:

$$E_e^{t_{sc},k} = \sum_{l=t_{sc-1}}^{t_{sc}} E_{P^k}^l - E_{D^k}^l - s \cdot \eta P_{B^k}^s. \tag{18}$$

B. Smart Contract

The smart contract coordinates the batteries operation so that they can share energy surpluses within the fleet, and in order to ensure that the aggregated net export in time interval t meets the contractual agreement E_c^t. Although a smart contract is not required and could be replaced by centralized operations realised by an centralized server, the smart contract increases the reliability and security of the coordination by removing single point of failure (which is of great importance in close to RTC), and by ensuring immunity to cyberattacks. Although smart contracts are not well adapted to full RTC with milliseconds time interval communication, the proposed algorithm relies on minutely to 15 minutes time intervals' communication between the assets and the smart contract, making it suitable for smart contract implementation.

In this study, a smart contract was implemented in an Ethereum based private blockchain using Ganache environment. The smart contract was developed using solidity, and compiled and deployed using Python's library web3.py. An aggregator account was defined and used to deploy and manage the smart contract and associated operating fees, as shown in Fig. 6. Similarly, each battery is associated with an account and is interacting with the smart contract using Python.

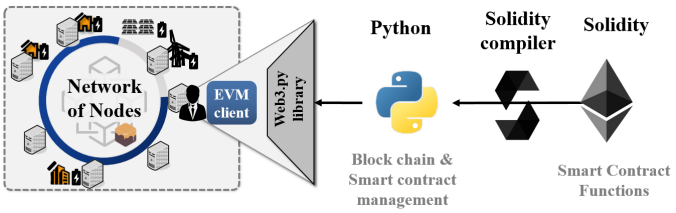

Fig. 6: Local Smart Contract implementation for distributed batteries coordination. The deployment and management of the smart contract is detailed for one node (the aggregator node).

The different functions implemented in the smart contract are the following:

- Constructor: to initialize the contract, that allows to define the address of the aggregator.
- Register a new household. This updates the smart contract mapping, and associates the household address to its current characteristics such as $SoC^{t_{sc},k}$, the last residual demand, and the last quantity of energy exported.
- Update the time series sent by the aggregator $(SoC^{t,A}, E_c^t, \mathcal{S}^t)$.
- Update an household information:
  - $SoC^{t_{sc},k}$ the battery SoC at the current time, $E_e^{t_{sc},k}$ the energy exported by household k since the last communication between the battery k and the smart contract,
  - the residual demand $E_{D^k}^{t_{s-1}} - E_{P^k}^{t_{s-1}}$,
  - a new variable $E_e^{t,k}$ that corresponds to the net exported energy of household k since the beginning of time interval t. It consists of the sum of all the previous quantities $E_e^{t_{sc},k}$.
- Compute the batteries weights w_i^k and w_e^k for all the batteries k. w_e^k is computed as follows:

$$w_e^k = \frac{W_e^k}{\sum_{k \in households} W_e^k} \tag{19}$$

where W_e^k is given as shown below:

$$W_e^k = \begin{cases} SoC^{t_{sc},k} & \text{if } E_e^{t_{sc},k} \geq 0 \text{ , } SoC^{t_{sc},k} \geq SoC^{t,A} \\ 0 & \text{Otherwise.} \end{cases} \tag{20}$$

Similarly, w_i^k is computed as follows:

$$w_i^k = \frac{W_i^k}{\sum_{k \in households} W_i^k} \tag{21}$$

where $W_i^k = 100\% - SoC^{t_{sc},k}$.

- Compute $RE^{t,A}$ the remaining aggregated energy to be exported:

$$RE^{t,A} = E_c^t - \sum_{k \in \text{households}} E_e^{t,k}. \tag{22}$$

This value could also be increased or reduced depending on a real-time frequency measurement to include frequency regulation and imbalance settlement aspects.
- Emit their information to all registered households: it allows the smart contract to send to every household the required information $RE^{t,A}, w_e^k, w_i^k, E_a$.

VI. Experimentation

A. Experimentation setup

The proposed algorithm was implemented for the use case described in section III. An aggregator invests in distributed residential generation assets (rooftop PV and micro Wind turbines), and in residential batteries that are all installed at customers premises. 70 households were considered in this study, each one of them with a micro-generation asset (solar PV or micro wind generation for a couple of households) and a residential battery [4]. To have a more general case, we consider that the aggregator already owns a Virtual Power Plant that includes one large PV power plant of 105 kW and one wind farm of 130 kW. The data used for the demand and production profiles used in the simulations are minutely data for all households from real measurements gathered within the ReFLEX project [53], but also from open sources [54]–[59]. The pricing data for the wholesale market price have been extracted from Nordpool's day-ahead market [60]. For the retail import price, we chose a dynamic ToU pricing scheme from [61]. Market time interval is 30 minutes. Hence, the day-ahead optimization uses time steps of 30 minutes. No intra-day optimization was realised for this work, although it would improve the revenues of the aggregator. Imbalance prices that apply to the aggregator when the net export energy differs from the contractual agreement, were extracted from [62]. Also, we consider that the whole fleet is linked by a virtual private wire contract [63], such that when an household consumes electricity that is produced by another asset of the fleet, the cost for this electricity quantity corresponds to 48 % of the retail electricity import price. This corresponds to the network costs with environmental and social obligations and taxes, as explained in Table I. Indeed, the energy production costs and supplier fees (operating costs, margin) can be discarded in this case [64]. Similarly, we do not consider any export tariff (such as FiT) for households, as this sort of incentive has already disappeared in many countries.

TABLE I: Breakdown of an electricity bill [64].

Bill component definition	**Value (%)**
Wholesale costs	33
Supplier Operation costs	18
Supplier margin	1
Supplier direct costs	2
Network costs	23
Environmental & social obligation costs	20
VAT	5

The communication time interval between the batteries and the smart contract is considered to be between 1 and 15 minutes. Finally, forecasts for the aggregated demand and production time series were generated using the real aggregated data multiplied by a random variable to account for uncertainties, as it will be discussed later. The time interval between two forecast values is also a parameter of the simulation considered to be between 30 min and 6 hours. All the optimizations and RTC algorithms were implemented on Matlab, whereas the smart contract was implemented and managed using Python, as explained in Fig. 6. The experimentation was conducted for a whole month.

B. Experimentation Results

The results presented in this section were obtained with a communication time interval of 5 minutes between the assets and the smart contract. The day-ahead demand and production forecasts time step for the aggregated fleet was 2 hours, with a simulated uncertainty of 25% around the real value. Hence, the simulation corresponds to a realistic and conservative case.

Fig. 7.a shows the wholesale market price that was used. Fig. 7.b displays the aggregated demand and production forecast, along with the fleet net energy export contracted in the

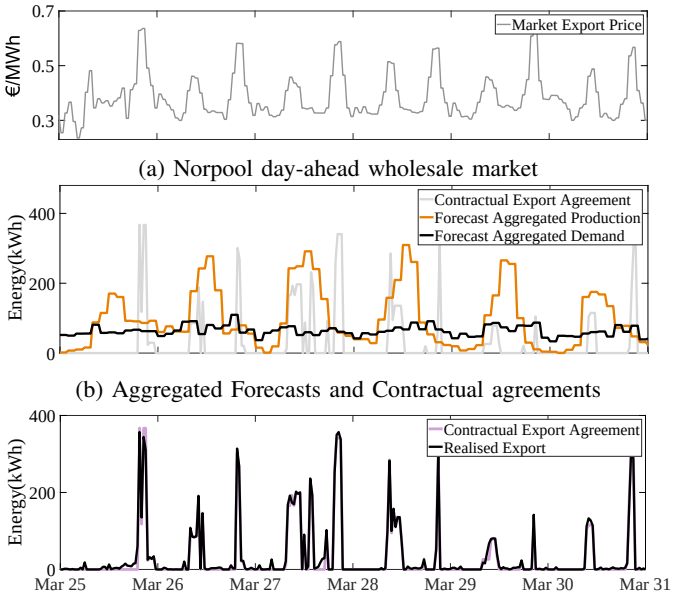

(a) Norpool day-ahead wholesale market

(b) Aggregated Forecasts and Contractual agreements

(c) Realised export from the whole fleet

Fig. 7: Experimental results displayed with time intervals of 30 minutes

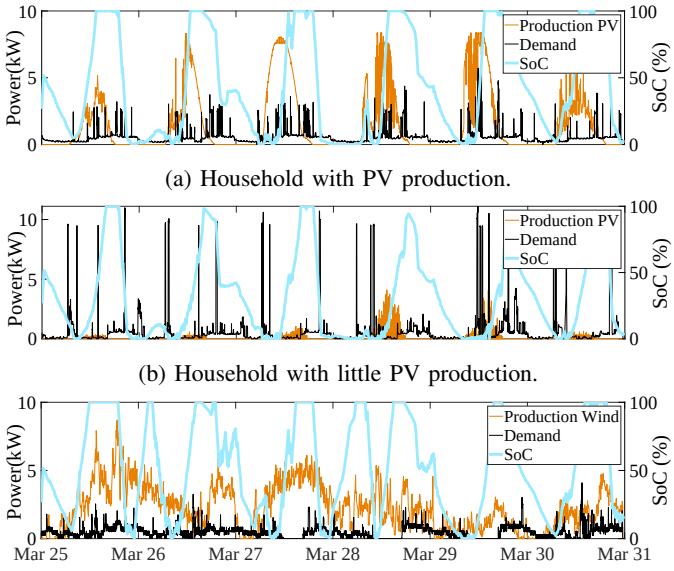

(a) Household with PV production.

(b) Household with little PV production.

(c) Household with micro-wind generation.

Fig. 8: Production, demand and resulting SoC for different households.

wholesale market, corresponding to the end of phase 2 as presented in Fig. 2. Finally, Fig. 7.c compares this contractual energy exports quantities with the actual realised export of the aggregated fleet. We can see that the achieved export quantities match the contractual export quantities. When the fleet's net export deviates from the agreed export, the aggregator pays an imbalance fee that is proportional to the deviation, and that depends on the system's frequency state at the moment of the deviation.

Then, Fig. 8 shows the real consumption and production data for three different households, along with the battery SoC that results from the RTC simulations. It shows that battery's SoC is following the local demand and production, as the SoC of the household with wind generation is different than the SoC of battery in households owning solar PV generation. Batteries' SoC also follows the aggregator and smart contracts recommendation in order to export the agreed energy quantities at the right time.

Using these simulations, it is possible to assess the economic benefits that an aggregator can expect from the proposed algorithm. The source of revenues for the aggregator are the bill reduction of the households and the revenues from the export of energy agreed on the wholesale market. The bill reduction is computed as the difference between the bill of an household before any asset was installed, and the bill of the same household implementing the same consumption profile after the assets are installed with the proposed algorithm. Also, the revenues from the wholesale market are subtracted by the imbalance costs that must be paid by the aggregator when the net export does not match the energy quantity from the contractual agreement. Different scenarios have been considered for comparison purpose:

- Scenario 0 (baseline): This scenario only considers the 70 households' demand, and assumes they do not have any distributed generation asset (no rooftop PV nor batteries). This is the baseline to compute the bill reduction.
- Scenario 1 (baseline with PV): idem as the previous scenario, with micro-generation installed at the consumers premises. No control algorithm is used in this scenario as there is no controllable asset.
- Scenario 2 (baseline with PV and independent battery control): idem as the previous scenario, with residential batteries installed, that do not implement the proposed algorithm, but an heuristic based algorithm. This heuristic algorithm simply charges the battery when the household produces more energy than it consumes, and discharges the battery when the household consumes more energy than it produces. It was shown in [7] that in a context of low or non existing export prices, this algorithm gives similar results to optimal local optimization based algorithms. However, this scenario does not consider any bidding on the whole sale market, nor any coordination or energy exchanges between batteries.
- Scenario 3 (VPP without battery but with all newly installed micro-generation assets at the same location): in this scenario, no households nor batteries are considered. It considers a general case where all the residential PV are installed by the VPP (aggregator) at the same location as the already owned VPP assets (PV power plant and wind farm). No control algorithm is used in this scenario as there are no controllable assets, and it is assumed that the VPP sells all the production at the day-ahead wholesale market price.
- Scenario 4 (VPP with all newly installed assets at the same location): similar to the previous scenario with all the residential batteries replaced by one large battery installed at the location of the VPP. This scenario im-

plements the proposed RT control algorithm considering only one aggregated battery with one large PV and wind power plant.

- Scenario 5 (Distributed residential assets): this scenario corresponds to the use case of this work: 70 residential loads with solar PV and a residential battery installed at each end-user premise. The solar PV and Wind farms already owned by the aggregator are also considered as distributed assets in the study.
- Scenario 6 (VPP with centralized assets and contract with households): this scenario corresponds to scenario 4, in which the aggregator also proposes a specific retail contract to the households, using the virtual private wire assumption. Hence, the production assets and batteries are installed in the same location, and the whole demand is seen by the aggregator as one large demand. However, when households consume electricity, they pay either the ToU tariff or a reduced tariff if they consume at time when the VPP assets are producing.

Table II displays the monthly bill for the 70 households in each scenario, along with the corresponding revenues for the aggregator (VPP). The revenue are computed as the sum between the bill reduction compared to the baseline (scenario 0) and the revenues from the export when assets are aggregated. No FiT was considered for households.

TABLE II: Comparison of economic benefits on a monthly basis of the proposed RT control algorithm.

Scenario	Aggregated Bills (€)	Market Revenue (€)	Aggregated Revenue (€)
0	6111	0	**0**
1	4984	0	**1127**
2	3853	0	**2258**
3	0	2676	**2676**
4	0	3025	**3025**
5	2903	891	**4100**
6	3201	909	**3820**

Table II shows that the proposed algorithm and use case provide the greatest revenues to the aggregator. It also shows that taking advantage of distributed (residential) production with the use of batteries for market bidding allows an aggregator or a VPP to increase its benefits by 7% compared to the scenario 6 in which the VPP invests in the same quantity of assets, but install them in a more centralized location, although the installation cost difference between these two scenarios is beyond the scope of the paper. This is due to the fact that in the case of centralized generation assets (scenario 6), the electricity importations from the households always include a network cost and taxes which do not apply in scenario 5 when households self-consume their production. Furthermore, these results were obtained for a conservative scenario considering forecast inaccuracy and communication time intervals of 5 minutes. This demonstrates the performance of the proposed RT algorithm that manages to take advantage of the local production while maximizing revenues from the wholesale market. Furthermore, using residential batteries with the proposed algorithm provide a revenue increase of 53 % compared to the case where the VPP only owns PV and wind farms in one location (scenario 3). This should incentivize investors to support the development of decentralized generation assets with an aggregator for market bidding. Finally, it can be seen from scenario 4 that the RT algorithm can also be implemented in the case of a single battery without any new development or change, which allowed an increase of the benefits for the VPP of 13%.

This study also shows that residential batteries used with the proposed algorithm increase greatly the self-consumption rate of end-users. Indeed, the average self-consumption of the individual households was increased from 28% in scenario 1 without batteries to 64% in scenario 4.

C. Sensitivity study of the algorithm

The algorithm proposed in this work relies on forecasts and close to RT communication between the assets and the smart contract. In this subsection, we propose to study the impact of forecast inaccuracy and communication time interval on the benefits of the algorithm.

1) Sensitivity to forecasts: Two forecasts parameters have been considered: the forecast accuracy and the time step within the forecast. Several simulations were run and averaged over a range of these two parameters. The forecast inaccuracy was assessed by multiplying the perfectly accurate forecast by a random variable uniformly distributed with different intervals such that forecast accuracy followed a range of 20 - 100% of accuracy. We considered time steps between two values of forecast ranging from 30 minutes to 6 hours. Aggregator revenues for the different ranges of these two parameters are displayed in Fig. 9. It shows that the forecast accuracy is the parameter that has the greatest impact on the revenue, as variations in the forecasts time step do not seem to have a clear influence on the aggregator's revenues. Furthermore, we can see that the proposed RT algorithm ensures that even with a minimum accuracy of 20 %, the revenues of the aggregator stay above 3300 €, and makes the distribution of micro-generation assets at customer premises with integration of households in the portfolio more profitable than a scenario 4 with perfect forecasts, in which the assets are installed in the same location, but without considering any household.

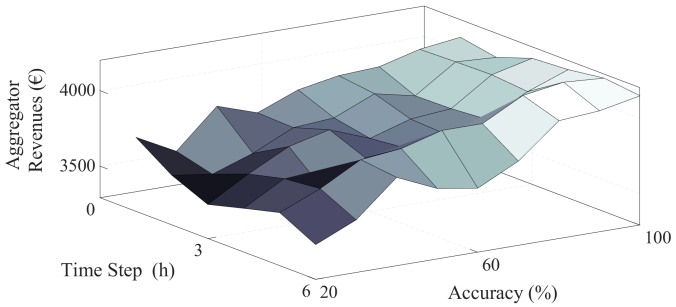

Fig. 9: Revenues of the aggregator obtained for different forecast accuracies and time steps.

2) Sensitivity to communication time interval: Simulations were run with different communication time interval between

the assets and the smart contract, ranging from 1 minute to 15 minutes. The resulting revenues for the aggregator are displayed in Fig. 10. We can see that communication time has a clear impact on the revenues, although communication time interval below 10 minutes maintain a monthly revenue above 4000 €for the aggregator.

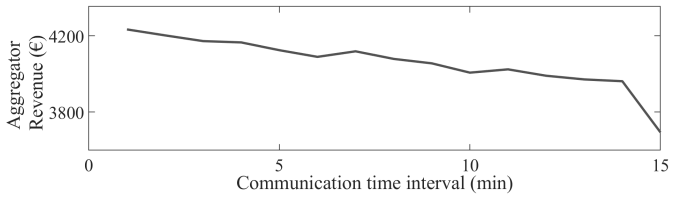

Fig. 10: Revenues of the aggregator obtained for different communication time intervals.

D. Impacts for the grid

Finally, although the RTC algorithm aims to limit the impact of the battery charging and discharging phases on the grid, this impact is not negligible. We can differentiate two main impacts on the grid: system level impacts, which are due to the characteristics of the profile of the aggregated fleet of assets, and affect mainly the frequency of the grid, and local impacts, which are due to single households load profiles, and are more likely to affect the local voltage.

1) System level: Fig. 11 shows the load profiles of the aggregated fleet in scenario 1 (that includes all the households demand, all the PV and wind generation, but no batteries) and in scenario 5 (that includes all the assets, with the batteries controlled by the RT control algorithm) for 1 minute and 30 minutes measurement time intervals. The load profile of the aggregated fleet with batteries is relatively flat when measured on a 30 minutes basis (Fig. 11.a), except for periods when export is incentivized by the grid. However Fig. 11.b shows that the actual profile is much more noisy due to the RT operations of the batteries that compensate for extra production or demand in order to meet the contractual agreements.

The monthly average power and Peak to Average Ratio (PAR) are displayed in Table III for both scenarios. We can see that the PAR has considerably increased in the case of batteries used to bid on the market. This is mostly due to an increase of the maximum power exported that occurs at time of high export prices, and to a decrease of the average power consumption in scenario 5. However, grid services such as frequency regulation were not addressed in this study, and might mitigate this impact. Therefore, although batteries help to balance the grid at critical times (times with a need for energy export), they could also increase the frequency variability within the market time intervals in a case of high penetration of batteries and low inertia of the grid.

2) Local level: Unlike the load profile of the aggregated households, at the local level, the variability of an household's load profile with batteries is comparable to its variability when there is no battery. Indeed, Fig. 12 shows the comparison of the PAR for every households before and after the installation of the batteries. Although the PAR for scenario 5 is slightly

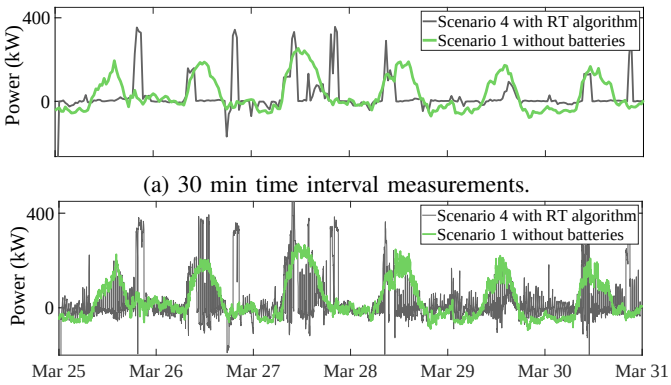

(a) 30 min time interval measurements.

(b) 1 min time interval measurements.

Fig. 11: Load profile of the aggregated fleet of assets for scenario 1 (which includes demand, solar PV and wind) and scenario 5 (demand, PV, wind and batteries with RT control). Fig.7, Fig. 8 and Fig. 11 should be redone on the same simulation so values are similar. They are different now because forecasts are different (accuracy $\neq$ 100%)

TABLE III: Average power and PAR for scenarios 1 and 5.

Scenario	Mean Power (kW)	PAR
1	19.8	14.8
5	11.7	46.9

greater than the PAR from scenario 1, the resulting PAR are comparable in both scenarios.

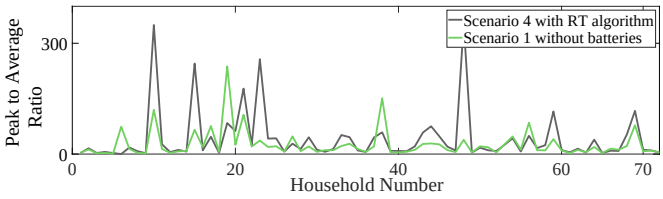

Fig. 12: Comparison of Peak to Average Ratio for scenario 1 and 5 for all considered households.

As an example, Fig. 13 shows the load profile of an household with and without batteries. We can see the displacement of production in order to follow the price incentive from the wholesale market. Therefore, similar to distributed solar PV (scenario 1), the use of batteries for wholesale market bidding would result in important local voltage increases if many batteries are located on the same primary transformer.

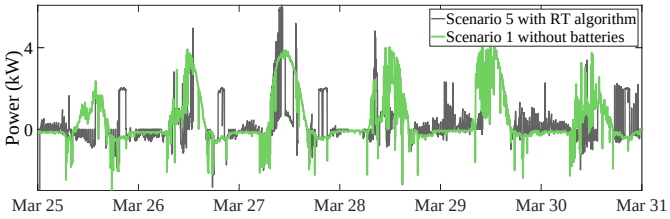

Fig. 13: Example of load profile comparison between scenario 1 and scenario 5 at a household level.

VII. Conclusion

This paper presented a real-time control algorithm for residential batteries that allows the battery owner to increase the revenues from the battery by bidding on the wholesale market. This algorithm is based on MPC to ensure that optimal decisions are taken locally, and is also based on a smart contract that securely coordinates a fleet of distributed batteries to meet the export agreements from the wholesale market. Considering a use case of 70 households with minutely consumption and production data, it was shown that the proposed algorithm increases the potential revenues for the owner of the residential batteries compared to a case where all the batteries are regrouped and installed in a central location. It also demonstrated that including residential flexible assets in the portfolio of aggregators makes it more profitable than a portfolio with only production power plants as it increases the revenues by 35%, and it ensures that more than 60% of the electric consumption will be produced from distributed renewable sources owned by the aggregator. Therefore, this algorithm provides new economic incentives to invest in decentralized renewable generation, which is necessary to meet the objectives of Net Zero Carbon emission schemes. The robustness of the algorithm to forecast errors and communication latency was also studied and validated. Finally, the impacts of this algorithm on the grid were also studied. Although these impacts are not negligible at the system level, they could be mitigated by including grid services in the batteries operations.

Acknowledgment

The authors would like to thank UKRI for funding...

References

[1] A. Adrees, J. V. Milanovic, and P. Mancarella, "Effect of inertia heterogeneity on frequency dynamics of low-inertia power systems," *IET Generation, Transmission Distribution*, vol. 13, DOI 10.1049/iet-gtd.2018.6814, no. 14, pp. 2951–2958, 2019.

[2] "Innovating to Net Zero: UK Net Zero Report," Energy Systems Catapult, Tech. Rep., 2020. [Online]. Available: https://es.catapult.org.uk/reports/innovating-to-net-zero/#

[3] "World Energy Outlook 2019," IEA, Tech. Rep., 2019. [Online]. Available: https://www.iea.org/reports/world-energy-outlook-2019

[4] "Powerwall, your home battery," 2019. [Online]. Available: https://www.tesla.com/sites/default/files/pdfs/powerwall/Powerwall%202_AC_Datasheet_en_GB.pdf

[5] "Lg solar batteries," 2019. [Online]. Available: https://www.lgenergy.com.au/products/battery

[6] C. Truong, M. Naumann, R. Karl, M. MÃ¼ller, A. Jossen, and H. Hesse, "Economics of residential photovoltaic battery systems in germany: The case of tesla's powerwall," *Batteries*, vol. 2, DOI 10.3390/batteries2020014, p. 14, 05 2016.

[7] B. Couraud, S. Norbu, M. Andoni, V. Robu, H. Gharavi,, and D. Flynn, "Optimal residential battery scheduling with asset lifespan consideration," in *2020 IEEE PES Innovative Smart Grid Technologies Europe (ISGT-Europe)*, pp. 1–5, 2020.

[8] S. van der Stelt, T. AlSkaif, and W. van Sark, "Techno-economic analysis of household and community energy storage for residential prosumers with smart appliances," *Applied Energy*, vol. 209, DOI https://doi.org/10.1016/j.apenergy.2017.10.096, pp. 266 – 276, 2018. [Online]. Available: http://www.sciencedirect.com/science/article/pii/S0306261917315337

[9] "Tesla applies for uk electricity provider licence," accessed June 2002. [Online]. Available: https://www.telegraph.co.uk/business/2020/05/02/tesla-applies-uk-electricity-provider-licence/

[10] "Autobidder," accessed June 2020. [Online]. Available: https://www.tesla.com/support/autobidder

[11] B. Mantar Gundogdu, D. T. Gladwin, S. Nejad, and D. A. Stone, "Scheduling of grid-tied battery energy storage system participating in frequency response services and energy arbitrage," *IET Generation, Transmission Distribution*, vol. 13, DOI 10.1049/iet-gtd.2018.6690, no. 14, pp. 2930–2941, 2019.

[12] J. Roldan-Perez, A. Rodriguez-Cabero, and M. Prodanovic, "Design and analysis of virtual synchronous machines in inductive and resistive weak grids," *IEEE Transactions on Energy Conversion*, vol. 34, DOI 10.1109/TEC.2019.2930643, no. 4, pp. 1818–1828, Dec. 2019.

[13] G. He, Q. Chen, and C. K. et. al., "Optimal bidding strategy of battery storage in power markets considering performance-based regulation and battery cycle life," *IEEE Transactions on Smart Grid*, vol. 7, DOI 10.1109/TSG.2015.2424314, no. 5, pp. 2359–2367, Sep. 2016.

[14] "The policy and regulatory context for new Local Energy Markets," Energy Systems Catapult, Tech. Rep., 2019. [Online]. Available: https://es.catapult.org.uk/reports/the-policy-and-regulatory-context-for-new-local-energy-markets

[15] H.-C. Gao, J.-H. Choi, S.-Y. Yun, H.-J. Lee, and S.-J. Ahn, "Optimal scheduling and real-time control schemes of battery energy storage system for microgrids considering contract demand and forecast uncertainty," *Energies*, vol. 11, DOI 10.3390/en11061371, no. 6, p. 1371, May. 2018. [Online]. Available: http://dx.doi.org/10.3390/en11061371

[16] J. M. Lujano-Rojas, R. Dufo-Lopez, J. L. Bernal-Agustin, and J. P. S. Catalao, "Optimizing daily operation of battery energy storage systems under real-time pricing schemes," in *2017 IEEE Manchester PowerTech*, pp. 1–1, 2017.

[17] G. Liu, Y. Xu, and K. Tomsovic, "Bidding strategy for microgrid in day-ahead market based on hybrid stochastic/robust optimization," *IEEE Transactions on Smart Grid*, vol. 7, no. 1, pp. 227–237, 2016.

[18] P. M. van de Ven, N. Hegde, L. MassouliÃ©, and T. Salonidis, "Optimal control of end-user energy storage," *IEEE Transactions on Smart Grid*, vol. 4, no. 2, pp. 789–797, 2013.

[19] A. S. Akyurek and T. S. Rosing, "Optimal distributed nonlinear battery control," *IEEE Journal of Emerging and Selected Topics in Power Electronics*, vol. 5, no. 3, pp. 1045–1054, 2017.

[20] M. Ruiz-Cortes, E. Gonzalez-Romera, R. Amaral-Lopes, E. Romero-Cadaval, J. Martins, M. I. Milanes-Montero, and F. Barrero-Gonzalez, "Optimal charge/discharge scheduling of batteries in microgrids of prosumers," *IEEE Transactions on Energy Conversion*, vol. 34, no. 1, pp. 468–477, 2019.

[21] K. Worthmann, C. M. Kellett, P. Braun, L. Grune, and S. R. Weller, "Distributed and decentralized control of residential energy systems incorporating battery storage," *IEEE Transactions on Smart Grid*, vol. 6, no. 4, pp. 1914–1923, 2015.

[22] M. Koller, T. Borsche, A. Ulbig, and G. Andersson, "Defining a degradation cost function for optimal control of a battery energy storage system," in *2013 IEEE Grenoble Conference*, pp. 1–6, 2013.

[23] D. Rosewater, A. Headley, F. A. Mier, and S. Santoso, "Optimal control of a battery energy storage system with a charge-temperature-health model," in *2019 IEEE Power Energy Society General Meeting (PESGM)*, pp. 1–5, 2019.

[24] P. Malysz, S. Sirouspour, and A. Emadi, "An optimal energy storage control strategy for grid-connected microgrids," *IEEE Transactions on Smart Grid*, vol. 5, no. 4, pp. 1785–1796, 2014.

[25] D. Jiang and W. Powell, "Optimal hour-ahead bidding in the real-time electricity market with battery storage using approximate dynamic programming," *INFORMS Journal on Computing*, vol. 27, DOI 10.1287/ijoc.2015.0640, 06 2015.

[26] C. Long, J. Wu, Y. Zhou, and N. Jenkins, "Peer-to-peer energy sharing through a two-stage aggregated battery control in a community microgrid," *Applied Energy*, vol. 226, DOI 10.1016/J.APENERGY.2018.05.097, 06 2018.

[27] G. He, Q. Chen, C. Kang, P. Pinson, and Q. Xia, "Optimal bidding strategy of battery storage in power markets considering performance-based regulation and battery cycle life," *IEEE Transactions on Smart Grid*, vol. 7, no. 5, pp. 2359–2367, 2016.

[28] G. Chasparis, M. Pichler, J. Spreitzhofer, and T. Esterl, "A cooperative demand-response framework for day-ahead optimization in battery pools," *Energy Informatics*, vol. 2, DOI 10.1186/s42162-019-0087-x, 09 2019.

[29] D. T. Nguyen and L. B. Le, "Optimal bidding strategy for microgrids considering renewable energy and building thermal dynamics," *IEEE Transactions on Smart Grid*, vol. 5, no. 4, pp. 1608–1620, 2014.

[30] H. Mohsenian-Rad, "Coordinated price-maker operation of large energy storage units in nodal energy markets," *IEEE Transactions on Power Systems*, vol. 31, no. 1, pp. 786–797, 2016.

[31] M. Kazemi, H. Zareipour, N. Amjady, W. D. Rosehart, and M. Ehsan, "Operation scheduling of battery storage systems in joint energy and ancillary services markets," *IEEE Transactions on Sustainable Energy*, vol. 8, no. 4, pp. 1726–1735, 2017.

[32] H. Mohsenian-Rad, "Optimal bidding, scheduling, and deployment of battery systems in california day-ahead energy market," *IEEE Transactions on Power Systems*, vol. 31, no. 1, pp. 442–453, 2016.

[33] H. Wang and B. Zhang, "Energy storage arbitrage in real-time markets via reinforcement learning," 11 2017.

[34] H. Mohsenian-Rad, "Optimal bidding, scheduling, and deployment of battery systems in california day-ahead energy market," *IEEE Transactions on Power Systems*, vol. 31, no. 1, pp. 442–453, 2016.

[35] J. Horta, E. Altman, M. Caujolle, D. Kofman, and D. Menga, "Real-time enforcement of local energy market transactions respecting distribution grid constraints," in *2018 IEEE International Conference on Communications, Control, and Computing Technologies for Smart Grids (SmartGridComm)*, pp. 1–7, 2018.

[36] S. S. Parvar, H. Nazaripouya, and A. Asadinejad, "Analysis and modeling of electricity market for energy storage systems," in *2019 IEEE Power Energy Society Innovative Smart Grid Technologies Conference (ISGT)*, pp. 1–5, 2019.

[37] R. Khatami, M. Parvania, and P. Khargonekar, "Continuous-time look-ahead scheduling of energy storage in regulation markets," DOI 10.24251/HICSS.2019.435, 01 2019.

[38] T. Zhao and Z. Ding, "Cooperative optimal control of battery energy storage system under wind uncertainties in a microgrid," *IEEE Transactions on Power Systems*, vol. 33, no. 2, pp. 2292–2300, 2018.

[39] P. Fortenbacher, J. L. Mathieu, and G. Andersson, "Modeling and optimal operation of distributed battery storage in low voltage grids," *IEEE Transactions on Power Systems*, vol. 32, no. 6, pp. 4340–4350, 2017.

[40] T. Morstyn, B. Hredzak, and V. G. Agelidis, "Control strategies for microgrids with distributed energy storage systems: An overview," *IEEE Transactions on Smart Grid*, vol. 9, no. 4, pp. 3652–3666, 2018.

[41] R. Zafar, J. Ravishankar, J. E. Fletcher, and H. R. Pota, "Multi-timescale model predictive control of battery energy storage system using conic relaxation in smart distribution grids," *IEEE Transactions on Power Systems*, vol. 33, no. 6, pp. 7152–7161, 2018.

[42] H. Nazaripouya, C. Chu, H. R. Pota, and R. Gadh, "Battery energy storage system control for intermittency smoothing using an optimized two-stage filter," *IEEE Transactions on Sustainable Energy*, vol. 9, no. 2, pp. 664–675, 2018.

[43] X. Qi, Y. Bai, H. Luo, Y. Zhang, G. Zhou, and Z. Wei, "Novel distributed optimal control of battery energy storage system in an islanded microgrid with fast frequency recovery," *Energies*, vol. 11, DOI 10.3390/en11081955, p. 1955, 07 2018.

[44] F. Sossan, E. Namor, R. Cherkaoui, and M. Paolone, "Achieving the dispatchability of distribution feeders through prosumers data driven forecasting and model predictive control of electrochemical storage," *IEEE Transactions on Sustainable Energy*, vol. 7, no. 4, pp. 1762–1777, 2016.

[45] J. Ospina, N. Gupta, A. Newaz, M. Harper, M. O. Faruque, E. G. Collins, R. Meeker, and G. Lofman, "Sampling-based model predictive control of pv-integrated energy storage system considering power generation forecast and real-time price," *IEEE Power and Energy Technology Systems Journal*, vol. 6, no. 4, pp. 195–207, 2019.

[46] E. Namor, F. Sossan, R. Cherkaoui, and M. Paolone, "Control of battery storage systems for the simultaneous provision of multiple services," *IEEE Transactions on Smart Grid*, vol. 10, no. 3, pp. 2799–2808, 2019.

[47] B. Xu, Y. Shi, D. S. Kirschen, and B. Zhang, "Optimal battery participation in frequency regulation markets," *IEEE Transactions on Power Systems*, vol. 33, no. 6, pp. 6715–6725, 2018.

[48] R. Zafar, J. Ravishankar, J. E. Fletcher, and H. R. Pota, "Optimal dispatch of battery energy storage system using convex relaxations in unbalanced distribution grids," *IEEE Transactions on Industrial Informatics*, vol. 16, no. 1, pp. 97–108, 2020.

[49] T. A. Nguyen, R. H. Byrne, B. R. Chalamala, and I. Gyuk, "Maximizing the revenue of energy storage systems in market areas considering non-linear storage efficiencies," in *2018 International Symposium on Power Electronics, Electrical Drives, Automation and Motion (SPEEDAM)*, pp. 55–62, 2018.

[50] M. Sufyan, N. Abd Rahim, M. Aman, C. Tan, and S. Raihan, "Sizing and applications of battery energy storage technologies in smart grid system: A review," *Journal of Renewable and Sustainable Energy*, vol. 11, DOI 10.1063/1.5063866, p. 014105, 02 2019.

[51] T. T. Teo, T. Logenthiran, W. L. Woo, and K. Abidi, "Near-optimal day-ahead scheduling of energy storage system in grid-connected microgrid," in *2018 IEEE Innovative Smart Grid Technologies - Asia (ISGT Asia)*, pp. 1257–1261, 2018.

[52] T. K. A. Brekken, A. Yokochi, A. von Jouanne, Z. Z. Yen, H. M. Hapke, and D. A. Halamay, "Optimal energy storage sizing and control for wind power applications," *IEEE Transactions on Sustainable Energy*, vol. 2, no. 1, pp. 69–77, 2011.

[53] "ReFLEX: Responsive FLEXibilities for Orkney Islands." [Online]. Available: http://www.emec.org.uk/ukri-gives-green-light-to-reflex-orkney-project-2/\

[54] R. Buswell, L. Webb, P. Cosar-Jorda, D. Marini, S. Brownlee, M. Thomson, S.-H. Yang, and R. Kalawsky, "Leedr project home energy dataset," Jul. 2018. [Online]. Available: https://repository.lboro.ac.uk/articles/dataset/LEEDR_project_home_energy_dataset/6176450/1

[55] J. Kolter and M. Johnson, "Redd: A public data set for energy disaggregation research," *Artif. Intell.*, vol. 25, 01 2011.

[56] B. A. Hebrail G., "Individual household electric power consumption Data Set," 2012. [Online]. Available: https://archive.ics.uci.edu/ml/datasets/Individual+household+electric+power+consumption

[57] S. Makonin, "RAE: The Rainforest Automation Energy Dataset," 2017. [Online]. Available: https://doi.org/10.7910/DVN/ZJW4LC

[58] S. Makonin, "ODDs: Occupancy Detection Dataset," 2015. [Online]. Available: https://doi.org/10.7910/DVN/2K9FFE

[59] M. A., "Open Power System Data," 2017. [Online]. Available: https://data.open-power-system-data.org/household_data/2017-11-10

[60] "Day-ahead market prices," 2020. [Online]. Available: https://www.nordpoolgroup.com/Market-data1/Dayahead/Area-Prices/ALL1/Hourly/?view=table

[61] "Agile Octopus," 2020. [Online]. Available: https://octopus.energy/agile/

[62] "System sell price and the system buy price," 2020. [Online]. Available: https://www.elexon.co.uk/knowledgebase/what-is-the-system-sell-price-and-the-system-buy-price/

[63] "A Review of potential commercial arrangements for facilitating 'Virtual Private Wire' grid connections," Community Energy Scotland, Smarter Grid Solutions, Scottish Power Energy Networks, Tech. Rep., 2017.

[64] "Energy companies' consolidated segmental statements," 2019. [Online]. Available: https://www.ofgem.gov.uk/data-portal/breakdown-electricity-bill

[65] H. Kim and K. G. Shin, "Scheduling of battery charge, discharge, and rest," in *2009 30th IEEE Real-Time Systems Symposium*, DOI 10.1109/RTSS.2009.38, pp. 13–22, Dec. 2009.

[66] M. Jongerden, B. Haverkort, H. Bohnenkamp, and J. Katoen, "Maximizing system lifetime by battery scheduling," in *2009 IEEE/IFIP International Conference on Dependable Systems Networks*, DOI 10.1109/DSN.2009.5270351, pp. 63–72, Jun. 2009.

[67] I. Duggal and B. Venkatesh, "Short-term scheduling of thermal generators and battery storage with depth of discharge-based cost model," *IEEE Transactions on Power Systems*, vol. 30, DOI 10.1109/TPWRS.2014.2352333, no. 4, pp. 2110–2118, Jul. 2015.

[68] D. Pelzer, D. Ciechanowicz, and A. Knoll, "Energy arbitrage through smart scheduling of battery energy storage considering battery degradation and electricity price forecasts," in *2016 IEEE Innovative Smart Grid Technologies - Asia (ISGT-Asia)*, DOI 10.1109/ISGT-Asia.2016.7796431, pp. 472–477, Nov. 2016.

[69] M. Kazemi and H. Zareipour, "Long-term scheduling of battery storage systems in energy and regulation markets considering battery's lifespan," *IEEE Transactions on Smart Grid*, vol. 9, DOI 10.1109/TSG.2017.2724919, no. 6, pp. 6840–6849, Nov. 2018.

[70] M. A. Ortega-Vazquez, "Optimal scheduling of electric vehicle charging and vehicle-to-grid services at household level including battery degradation and price uncertainty," *IET Generation, Transmission Distribution*, vol. 8, DOI 10.1049/iet-gtd.2013.0624, no. 6, pp. 1007–1016, Jun. 2014.

[71] J. Dulout, A. Luna Hernandez, A. Anvari-Moghaddam, C. Alonso, J. Guerrero, and B. Jammes, "Optimal scheduling of a battery-based energy storage system for a microgrid with high penetration of renewable sources," 07 2017.

[72] D. Liu, Y. Xu, Q. Wei, and X. Liu, "Residential energy scheduling for variable weather solar energy based on adaptive dynamic programming," *IEEE/CAA Journal of Automatica Sinica*, vol. 5, DOI 10.1109/JAS.2017.7510739, no. 1, pp. 36–46, Jan. 2018.

[73] M. R. et. al., "Optimal charge/discharge scheduling of batteries in microgrids of prosumers," *IEEE Trans. on Energy Conversion*, vol. 34, DOI 10.1109/TEC.2018.2878351, no. 1, pp. 468–477, Mar. 2019.

[74] Y. Yoon and Y.-H. Kim, "Charge scheduling of an energy storage system under time-of-use pricing and a demand charge," *TheScientificWorldJournal*, vol. 2014, DOI 10.1155/2014/937329, 07 2014.

[75] A. Bouakkaz and et. al., “Optimal scheduling of household appliances in off-grid hybrid energy system using PSO algorithm for energy saving,” 03 2019.